

Fast Uncertainty Quantification for Kernel-Based Estimators in Large-Scale Causal Inference

Matthew Kosko*

Department of Population Health, New York University,
New York, NY, 10016

Falco J. Bargagli-Stoffi[†]

Department of Biostatistics, University of California,
Los Angeles, CA,

Lin Wang

Department of Statistics, Purdue University,
West Lafayette, IN 47907,

and

Michele Santacatterina[‡]

Department of Population Health, New York University,
New York, NY, 10016

March 17, 2026

*Corresponding author: Matthew.Kosko@nyulangone.org.

[†]This article is based upon work supported by The Amazon Web Services (AWS) funding for “AI/ML for Identifying Social Determinants of Health”.

[‡]This article is based upon work supported by the National Science Foundation under Grant No 2306556, and the National Institute of Health Grant No 1R01AI197146-01.

Abstract

Kernel methods are widely used in causal inference for tasks such as treatment effect estimation, policy evaluation, and policy learning. The bootstrap is a standard tool for uncertainty quantification because of its broad applicability. As increasingly large datasets become available, such as the 2023 U.S. Natality data from the National Vital Statistics System (NVSS), which includes 3,596,017 registered births, the computational demands of these methods increase substantially. Kernel methods are known to scale poorly with sample size, and this limitation is further exacerbated by the repeated re-fitting required by the bootstrap. As a result, bootstrap-based inference for kernel-based estimators can become computationally infeasible in large-scale settings. In this paper, we address these challenges by extending the causal Bag of Little Bootstraps (cBLB) algorithm to kernel methods. Our approach achieves computational scalability by combining subsampling and resampling while preserving first-order uncertainty quantification and asymptotically correct coverage. We evaluate the method across three representative implementations: kernelized augmented outcome-weighted learning, kernel-based minimax weighting, and double machine learning with kernel support vector machines. We show in simulations that our method yields confidence intervals with nominal coverage at a fraction of the computational cost. We further demonstrate its utility in a real-world application by estimating the effect of any amount of smoking on birth weight, as well as the optimal treatment regime, using the NVSS dataset, where the standard bootstrap is prohibitively expensive computationally and effectively infeasible at this scale.

Keywords: causal bootstrap; real-world data; propensity score; covariate balance; machine learning

1 Introduction

Kernel methods represent a versatile class of algorithms that enable powerful nonparametric modeling, and they have become essential tools across multiple areas of causal inference. Applications include modeling treatment effect heterogeneity (Imai & Ratkovic 2013), learning optimal treatment policies (Zhao et al. 2012, Zhou & Kosorok 2017, Zhou et al. 2017), estimating kernel minimax weights to correct for covariate imbalance (Kallus et al. 2021, Kallus & Santacatterina 2022, Hirshberg & Wager 2021), estimating nuisance functions in doubly robust estimators (Naimi & Kennedy 2017), and estimating dose-response curves (Singh et al. 2024, Kennedy et al. 2017). These methods operate by mapping data into high-dimensional feature spaces, enabling the use of linear operations to capture complex nonlinear relationships. We provide additional details on the central role of kernel methods in these approaches in Section 1.3.

The bootstrap methodology (Efron 1979, Efron & Tibshirani 1994) has been used to calculate precision estimates for statistical estimators, such as standard errors and confidence intervals. The literature on the bootstrap’s use in causal inference, particularly for large datasets, is still relatively sparse (see Kosko et al. (2024) and section 1.3 below).

The need to scale both estimation and inference methods is increasingly pressing, as researchers are collecting and analyzing ever-larger observational and experimental datasets to infer causal effects. For example, Bargagli-Stoffi et al. (2020) and Wu et al. (2024) used data on over 35 million Medicare beneficiaries across the US to study heterogeneous treatment effects and estimate average causal exposure-responses, respectively. Nazaret & Sapiro (2023) analyzed 76 billion minutes of Apple Watch activity data from 160,000 users to evaluate a standing nudge (hourly alert to stand) using a regression discontinuity design (RDD). de Bont et al. (2024) conducted a multi-city Indian study on air quality and mor-

tality, leveraging 3.6 million death records across 10 cities (2008–2019) using instrumental variables (IV) to isolate the effect of locally generated PM2.5 pollution on deaths.

Despite their usefulness, neither kernel methods nor the bootstrap scale well to large datasets. Although increased computing power has made the bootstrap more accessible, it remains computationally burdensome when applied to large datasets, particularly in settings that require complex resampling procedures. To overcome these challenges, Kleiner et al. (2014) proposed the bag of little bootstraps (BLB), which, instead of applying an estimator to a smaller subsample, deploys the bootstrap on multiple subsets or “bags” of the data. Finally, BLB draws bootstrap samples equal to the size of the full dataset. While BLB improves the bootstrap’s efficiency, it was not introduced as a method for quantifying the precision of causal effect estimators. Kosko et al. (2024) introduced a new bootstrap algorithm called causal bag of little bootstraps (cBLB) for estimating average treatment effects with large data. The authors used a weighted version of the BLB to obtain estimates of uncertainty for variance-stabilized IPW estimators using weights obtained by logistic regression, covariate balancing propensity score (CBPS) (Imai & Ratkovic 2014), and machine learning. Kosko et al. (2024) showed that their proposed method significantly enhances the computational efficiency of the traditional bootstrap while maintaining consistent estimation of the average treatment effect from large datasets.

Although recent advances, such as cBLB, offer promising results, they still inherit many limitations of traditional approaches. In particular, they are susceptible to bias under model misspecification (Kang & Schafer 2007), may yield invalid inferences when using flexible, data-adaptive methods (Naimi et al. 2023), and can lead to erroneous inferences under lack of overlap (Kallus et al. 2021). In addition, the computational complexity only increases with the use of kernels. As is well-known, these kernel-methods are computationally-intensive with large datasets and there has been increasing interest in how to scale these

methods (Kim et al. 2023)

1.1 Contribution

Our work is motivated by the increasing usage of the bootstrap to construct confidence intervals in the context of causal inference with large real-world data using flexible kernel methods and accounts for the shortcoming of cBLB approaches. In particular, we contribute to this area of research by introducing a new bootstrap algorithm that significantly improves the computational efficiency of the standard nonparametric bootstrap for calculating standard errors and confidence intervals of kernel-based estimators. Our approach builds upon and extends the work of Kleiner et al. (2014) and Kosko et al. (2024) on bag of little bootstrap algorithms for statistical and causal inference estimators.

Our approach, which we call the causal bag of little bootstraps (cBLB), replaces full-sample bootstrap refitting with a subsampling-and-resampling scheme tailored to kernel estimators. We first randomly partition the full dataset into s disjoint bags of size $b \ll n$, with b chosen so that kernel fitting remains computationally feasible. Within each bag, we fit the kernel-based estimator (and any required nuisance models or optimization problems) once, compute per-observation contributions that can be re-aggregated under resampling weights, and then hold these fitted objects fixed across the r bootstrap replicates for that bag. These contributions may be influence-function/score terms for AIPW/DML-type estimators or weighted loss/residual terms for kernelized policy learning. We then generate r bootstrap replicates by drawing multinomial counts $M_1, \dots, M_b \sim \text{Multinomial}(n; \frac{1}{b}, \dots, \frac{1}{b})$ and forming the bootstrap replicate as the weighted average $\hat{\theta}^{*(\ell)} = \frac{1}{n} \sum_{a=1}^b M_a \hat{\theta}_{i_a}$, which mimics an n -out-of- n nonparametric bootstrap without recomputing kernels or refitting models. Finally, we construct confidence intervals within each bag, for example percentile intervals across the r replicates, and aggregate across bags by averaging the bag-specific

quantiles, yielding a scalable approximation to full-bootstrap uncertainty.

Through Monte Carlo simulations, we show that the proposed method substantially improves computational efficiency while maintaining nominal finite-sample coverage, consistent with the first-order uncertainty quantification and asymptotically correct coverage established by our theory. We evaluate the method across three representative implementations: optimal policy learning via kernelized augmented outcome-weighted learning (AOL) Zhou & Kosorok (2017), kernel-based minimax weighting Hirshberg & Wager (2021), and double machine learning (DML) with kernel support vector machines (SVMs) Kennedy (2022). These three different methods represent a range of kernel-based approaches used in causal inference, and they allow us to demonstrate the versatility and robustness of our proposed method across different settings. In all cases, our method yields confidence intervals with nominal coverage at a fraction of the computational cost. In addition, we provide the R code for the algorithm at <https://github.com/mdk31/kernel-blb>.

1.2 Smoking and Birthweight in the NVSS: A Setting Where the Standard Bootstrap is Computationally Prohibitive

We demonstrate our proposed method using the 2023 National Vital Statistics System (NVSS) natality dataset, which contains 3,596,017 registered singleton live births in the United States (National Center for Health Statistics 2024). The dataset includes detailed information on maternal sociodemographic characteristics, prenatal care, health behaviors including trimester-specific smoking status, and infant outcomes including birthweight. This setting is compelling for two reasons. First, the well-characterized causal effect of smoking on birthweight provides a credible benchmark against which to evaluate our estimators: we expect negative effects of plausible magnitude (research shows reductions on

the order of 150–250 grams (Hellerstedt et al. 1997, Wisborg et al. 2001, Adegboye et al. 2010, Cattaneo 2010)). Second, the scale of the dataset is precisely the regime in which standard bootstrap inference becomes computationally infeasible, motivating the need for scalable resampling alternatives such as the one proposed.

In this motivating application, we estimate distinct causal quantities using our proposed methods. The kernel minimax weights and DML with SVMs approaches both estimate the average treatment effect of smoking during pregnancy on birthweight. The AOL approach instead learns an optimal treatment regime. This means to learn a decision rule mapping maternal characteristics to a smoking recommendation. Given the overwhelming evidence of harm, we expect the estimated average treatment effects to be negative and of plausible magnitude, and the learned regime to universally recommend abstinence from smoking, with the corresponding optimal value reflecting the mean birthweight in a population following this recommendation.

We emphasize that the purpose of this application is not to find new results, but rather to provide a credible validation of our methods against a well-understood ground truth. Using this dataset, we estimate causal effects and construct confidence intervals via our proposed cBLB procedure, demonstrating its practical utility for scalable causal inference in large-scale observational studies, where the standard bootstrap is prohibitively expensive computationally and effectively infeasible at this scale.

1.3 Related Work

Kernel methods have been widely used in personalized medicine and optimal policy learning. Optimal policy learning seeks to develop decision rules that recommend treatments based on individual characteristics to maximize expected outcomes. This approach, also known as personalized medicine or individualized treatment rules (ITRs), acknowledges

that individuals may respond differently to the same treatment, making personalization essential for optimal care (Zhao et al. 2012). Several methodological frameworks have emerged in the optimal policy learning literature. One is the transformation of treatment regime estimation into a weighted classification problem using kernel machines, as demonstrated by outcome weighted learning (OWL) Zhao et al. (2012). OWL typically employs SVMs with kernel functions to flexibly model nonlinear treatment decision boundaries. To address some limitations of OWL—such as sensitivity to outcome shifts and its inability to handle negative outcomes—residual weighted learning (RWL) was proposed Zhou et al. (2017). RWL also relies on kernel-based classification but replaces outcome weights with residuals from regression models, improving robustness and finite-sample performance Zhou & Kosorok (2017). Building on OWL and RWL, Fu et al. (2019) developed Robust OWL (ROWL), which improves the stability of kernel-based treatment rules by using bounded, non-convex loss functions within the same learning framework. Another extension is Augmented OWL (AOL) by Zhou & Kosorok (2017), which incorporates outcome regression through augmented inverse probability weighting while preserving the kernel-based classification structure. This achieves semiparametric efficiency and avoids the non-convex optimization required by RWL.

Kernel methods naturally quantify distributional similarity through reproducing kernel Hilbert space (RKHS) embeddings (Hirshberg & Wager 2021, Ben-Michael et al. 2021, Kallus 2020), making them well-suited for covariate balancing methods that aim to estimate weights which balance covariate distributions across groups (Ben-Michael et al. 2021). For example, Kallus (2020) proposed a unifying framework that formulates matching and weighting as the problem of minimizing worst-case bias over a specified function class. They showed that several existing methods—including exact matching and propensity score weighting—can be interpreted as minimizing bias under different func-

tion classes, and introduced new kernel-based estimators that minimize worst-case bias in an RKHS. Subsequent work extended this framework to more complex settings, including marginal structural models, average treatment effects, and continuous exposures (Kallus et al. 2021, Kallus & Santacatterina 2022, Santacatterina & Kallus 2021, Kallus & Santacatterina 2019). In particular, Kernel Optimal Orthogonality Weighting (KOOOW) (Kallus & Santacatterina 2019) minimizes the worst-case functional covariance between the treatment variable and confounders in an RKHS, while incorporating a regularization term to avoid extreme weights. Recent work has also addressed the computational bottleneck of kernel balancing in very large datasets by using the rank-restricted Nystöm method to compute a kernel basis for balancing in nearly linear time and space, combined with scalable convex optimization for the weights Kim et al. (2023). While this is an important contribution, it focuses on making a specific kernel weighting estimator scalable, whereas our proposed method makes bootstrap-based uncertainty quantification scalable for a broader class of kernel-based estimators.

Kernel methods also appear in the DML framework, a modern approach that uses machine learning for estimating nuisance functions while achieving unbiased, \sqrt{n} -consistent estimates of causal parameters (Chernozhukov et al. 2017). The idea behind DML is to estimate nuisance functions (e.g., the outcome $m(x) = E[Y|X = x]$ or propensity score $\pi(x) = P[W = 1|X = x]$) with flexible methods, then form an orthogonalized estimating equation so that the first-order error in nuisance estimates does not bias the target parameter. Additionally, DML uses sample-splitting or cross-fitting to avoid regularization biases (Chernozhukov et al. 2017, Kennedy 2023). In this framework, any regression method achieving a sufficient rate of convergence can be used for the nuisances – including kernel-based learners. For instance, Naimi & Kennedy (2017) used a SuperLearner ensemble that included a SVM to estimate nuisance functions. Additionally, Colangelo & Lee

(2020) applied kernel-based double debiased machine learning estimators to estimate the effect of a continuous treatment.

When the bootstrap is used in causal inference, it typically involves drawing samples with replacement from the data and “re-designing” each sample to maintain covariate balance (Zhang & Sabbaghi 2021, Dagan et al. 2021). There is more work on the bootstrap in the context of matching estimators; both Abadie & Imbens (2008) and Abadie & Spiess (2022) explored applying the bootstrap to matching. Abadie & Imbens (2008) highlights that the standard bootstrap does not provide valid inference for matching estimators, requiring adjustments. Building on this, Abadie & Spiess (2022) investigates how to compute valid standard errors for regression coefficients, including treatment effects, post-matching. Similarly, Otsu & Rai (2017) addresses the issues raised by Abadie & Imbens (2008) by developing a weighted bootstrap that does not count how many times an observation is used in estimating the bootstrap statistic, instead resampling observations directly. Adusumilli (2018) introduces a modified bootstrap approach based on the concept of potential errors, while Zhao et al. (2019) applies the bootstrap to sensitivity analysis, providing confidence intervals for such analyses.

Paper Organization. The remainder of this paper is organized as follows. In Section 2, we provide a detailed description of the kernel-based methods we consider in our simulation experiments and real-world application. In Section 3, we introduce our proposed method for fast uncertainty quantification for kernel-based estimators in large-scale causal inference and discuss some properties. In Section 4, we present the results of our Monte Carlo simulation studies evaluating the performance of our method across different settings and provide practical guidelines informed by these empirical results. In Section 5, we apply our method to the NVSS dataset to estimate the effect of smoking on birthweight and learn an optimal treatment regime. Finally, in Section 6, we discuss the implications

of our findings, limitations of our approach, and directions for future research.

2 Setup: Kernel-based Estimators for Treatment Effect Estimation and Policy Learning

As described above, kernel methods are versatile tools used across a range of causal inference tasks. In this paper, we focus on three representative kernel-based methods that serve as case studies for our simulation experiments and real-world application. Specifically, we consider: (1) a kernelized version of the Augmented Outcome-Weighted Learning (AOL) method for estimating optimal treatment regimes (Zhou & Kosorok 2017); (2) a covariate balancing estimator using kernel minimax weights within the Augmented Minimax Linear Estimation framework (Hirshberg & Wager 2021); and (3) a DML estimator that employs kernelized SVM to learn nuisance functions (Kennedy 2022).

2.1 Kernelized Augmented Outcome-Weighted Learning

The goal of optimal treatment regime estimation is to learn a decision rule that maps patient covariates X to a treatment assignment $A \in \{-1, +1\}$ in order to maximize expected clinical outcomes. AOL frames this problem as a weighted classification task, where the misclassification loss is weighted by counterfactual residuals derived from a doubly robust estimator. While linear decision functions are computationally attractive, they may fail to capture complex, nonlinear treatment boundaries in high-dimensional covariate spaces.

To address this, AOL can be extended to a nonlinear setting by modeling the decision function $f(x)$ in a reproducing kernel Hilbert space (RKHS). Specifically, the decision rule is parameterized as $f(x) = h(x) + b$, where $h \in \mathcal{H}_K$ and \mathcal{H}_K is the RKHS associated with

a Mercer kernel $K(\cdot, \cdot)$. The learning objective is then to minimize a regularized empirical risk, with a convex surrogate loss applied to the sign-adjusted decision margin:

$$\min_{h \in \mathcal{H}_K, b \in \mathbb{R}} \frac{1}{n} \sum_{i=1}^n \frac{|\tilde{r}_i|}{\pi(a_i, x_i)} \phi(a_i \cdot \text{sign}(\tilde{r}_i) \cdot (h(x_i) + b)) + \frac{\lambda}{2} \|h\|_{\mathcal{H}_K}^2,$$

where $\phi(\cdot)$ is a convex surrogate loss (e.g., Huberized hinge loss), and \tilde{r}_i denotes the counterfactual residual for observation i .

By the representer theorem, the solution $h(\cdot)$ admits the finite representation $h(x) = \sum_{j=1}^n v_j K(x, x_j)$, converting the infinite-dimensional problem into a finite-dimensional convex optimization over coefficients $\{v_j\}$ and bias b . This formulation enables AOL to learn flexible, nonlinear treatment regimes while retaining global convergence guarantees and computational efficiency via standard solvers such as L-BFGS.

Despite its flexibility, kernelized AOL introduces computational challenges that scale with the number of training examples. Specifically, the kernel representation requires storing and manipulating the full $n \times n$ Gram matrix, leading to $\mathcal{O}(n^2)$ memory complexity in optimization scenarios. This issue can become prohibitive in large datasets.

2.2 Kernel Minimax Weights

For both the covariate balancing estimator using kernel minimax weights and the DML approach employing support vector machines to estimate nuisance functions, we focus, for simplicity, on estimands such as the average treatment effect, $\mathbb{E}[Y(1) - Y(0)]$. Specifically, we consider $\mathbb{E}[Y(a)]$, which is nonparametrically identified under standard causal inference assumptions (ignorability, positivity, and consistency) as

$$\mathbb{E}[Y(a)] = \mathbb{E}[\mathbb{E}[Y \mid A = a, X]] = \mathbb{E}[m_a(X)] = \Psi(m_a).$$

We define $Y_i = m_a(X_i) + \epsilon_i$, which implies $\epsilon_i = Y_i - m_a(X_i)$ and $m_a(X_i) = Y_i - \epsilon_i$ where

$\mathbb{E}[\epsilon_i | x_i] = 0$, and $\sigma^2 = \mathbb{E}[\epsilon_i^2 | A_i = a, X_i] = \text{Var}[Y_i | A_i = a, X_i]$ for $a = 0, 1$ and all i . Let $\delta_{m_a}(X_i) = \hat{m}_a(x_i) - m_a(X_i)$ (the regression error) and recall the augmented estimator for treatment a we considered

$$\begin{aligned}\hat{\Psi}^a &= \frac{1}{n} \sum_{i=1}^n \hat{m}_a(X_i) \\ &\quad - \frac{1}{n} \sum_{i=1}^n [\gamma(A_i, X_i)(\hat{m}_a(X_i) - Y_i)],\end{aligned}$$

where $\gamma(A_i, X_i) = \mathbb{I}[\{A_i = a\}]\gamma(X_i)$ and where $\gamma(X_i)$ could be chosen to be set to $\frac{1}{\pi(X_i)}$ as in section 2.3 below. By looking at the error of this estimator we can decompose this estimator as

$$\begin{aligned}\hat{\Psi}^a - \Psi(m_a) &= \frac{1}{n} \sum_{i=1}^n [(\delta_{m_a}(X_i) + m_a(X_i))] \\ &\quad - \frac{1}{n} \sum_{i=1}^n [\gamma(A_i, X_i)\delta_{m_a}(X_i)] \\ &\quad + \frac{1}{n} \sum_{i=1}^n [\gamma(A_i, X_i)\epsilon_i] - \Psi(m_a) \\ &= \frac{1}{n} \underbrace{\left[\sum_{i=1}^n \delta_{m_a}(X_i) - \sum_{i=1}^n \gamma(A_i, X_i)\delta_{m_a}(X_i) \right]}_{\text{imbalance in } \delta_{m_a}} \\ &\quad + \underbrace{\frac{1}{n} \sum_{i=1}^n \gamma(A_i, X_i)\epsilon_i}_{\text{noise - mean zero}} + \underbrace{\frac{1}{n} \sum_{i=1}^n m_a(X_i) - \Psi(m_a)}_{\text{sampling variation - mean zero}}\end{aligned}$$

We assume that $\delta_{m_a}(X_i)$ is contained in an absolutely convex set of functions \mathcal{M} (i.e. a Hilbert Space).

We then choose $\gamma(A_i, X_i)$ controlling the maximal imbalance in \mathcal{M} . In formulas we consider the following worst imbalance in \mathcal{M}_a ,

$$\mathbb{I}_{\mathcal{M}_a}(\gamma) = \sup_{\delta_{m_a} \in \mathcal{M}} \left| \frac{1}{n} \left(\sum_{i=1}^n \delta_{m_a}(X_i) - \sum_{i=1}^n \gamma(A_i, X_i) \delta_{m_a}(X_i) \right) \right|$$

Typically, $\gamma(A_i, X_i)$ is obtained by minimizing the worst-case imbalance while accounting for some measure of the complexity of the weights, ie., $\frac{\sigma^2}{n^2} \sum_i \mathbb{I}[(V_i = v, S_i = 1) \gamma(A_i, X_i, V_i)]^2$, where σ^2 . Following standard practice (Hirshberg & Wager 2021, Kallus & Santacatterina 2022), we choose as a model \mathcal{M}_a the unit ball $\mathcal{B}_{\mathcal{H}} = \{m_a(x) \in \mathcal{H} : \|m_a\|_{\mathcal{H}} \leq 1\}$ of an RKHS \mathcal{H} . Define the matrix $K_a \in \mathbb{R}^{n \times n}$ as $K_{aij} = \mathcal{K}_a(X_i, X_j)$ and setting $\gamma_i = \gamma(X_i)$ for convenience. By the representer theorem, we have that

$$\begin{aligned} \mathbb{I}_{\mathcal{M}_a}(\gamma) &= \sup_{\|m_a\|_{\mathcal{H}}^2 \leq 1} \left(\frac{1}{n} \sum_{i=1}^n (1 - \mathbb{I}[\![A_i = a]\!] \gamma_i) m_a(X_i) \right)^2 \\ &= \sup_{\sum_{i,j=1}^n \alpha_i \alpha_j \mathcal{K}_a(X_i, X_j) \leq 1} \left(\frac{1}{n} \sum_{i=1}^n (1 - \mathbb{I}[\![A_i = a]\!] \gamma_i) \sum_{j=1}^n \alpha_j \mathcal{K}_a(X_i, X_j) \right)^2 \\ &= \sup_{\alpha^T K_a \alpha \leq 1} \left(\frac{1}{n} \alpha^T K_a (e_n - I_a \gamma) \right)^2 \\ &= \frac{1}{n^2} (I_a \gamma - e_n)^T K_a (I_a \gamma - e_n) \\ &= \frac{1}{n^2} (\gamma^T I_a K_a I_a \gamma - 2 e_n^T K_a I_a \gamma + e_n^T K_a e_n) \end{aligned}$$

where e_n is the length- n vector with observations equal to 1, and I_a is the n -by- n diagonal matrix with $\mathbb{I}[\![A_i = a]\!]$ in the i^{th} diagonal entry. This leads to the following optimization problem

$$\hat{\gamma} = \arg \min_{\gamma} \left[\mathbb{I}_{\mathcal{M}}^2(\gamma) + \lambda \frac{\sigma^2}{n^2} \sum_i \gamma(A_i, X_i, V_i)^2 \right],$$

where λ is an arbitrary penalization parameter, and

$$\mathbb{I}_{\mathcal{M}}^2(\gamma) = \mathbb{I}_{\mathcal{M}_1}^2(\gamma) + \mathbb{I}_{\mathcal{M}_0}^2(\gamma).$$

Finally, the obtained weights $\hat{\gamma}$ are then plugged into the augmented estimator $\hat{\Psi}^a$. Similar to AOL, this introduces computational challenges that scale with the number of training examples, making uncertainty calculations with standard bootstrap computationally prohibitive in large datasets.

2.3 Double Machine Learning with Support Vector Machines

Estimating treatment effects via DML involves constructing an orthogonalized moment function (score) that enables robust, unbiased estimation of targets like the average treatment effect (ATE) or conditional ATE (CATE) while using flexible machine learning to learn nuisance functions (Chernozhukov et al. 2017, Kennedy 2023). The key property is Neyman orthogonality (or pathwise differentiability), which means the moment condition is insensitive to small errors in the nuisance estimates (Chernozhukov et al. 2017).

This framework yields augmented estimators in the form of $\hat{\Psi}^a$ defined in Section 2.2 with desirable properties (Chernozhukov et al. 2017, Rotnitzky et al. 2021). Implementation requires estimating the nuisance functions $(\hat{\pi}, \hat{m}_a)$ using flexible learners, and employs sample-splitting (cross-fitting) to avoid overfitting biases (Chernozhukov et al. 2017, Robins et al. 2008). In cross-fitting, the sample is partitioned into K folds; for each fold, the nuisance models are trained on the other $K - 1$ folds and then used to compute the moment function on the held-out fold

In this work, we use kernel-based SVMs to learn the propensity score $\pi(X)$ and outcome regressions $m_a(X)$ within the DML procedure. SVMs are appealing as first-stage learners

because they provide a flexible nonparametric fit while enforcing regularization via convex loss minimization. There are, however, important computational considerations when using kernel SVMs in a cross-fitted DML. In popular implementations of SVMs as in scikit-learn, an SVM’s time complexity scales between $\mathcal{O}(n_{\text{features}} \times n^2)$ and $\mathcal{O}(n_{\text{features}} \times n^3)$, making uncertainty calculations with standard bootstrap computationally infeasible for large datasets. (Pedregosa et al. 2011, Chapelle 2007).

3 Causal Bag of Little Bootstraps

We observe i.i.d. data $Z_i = (Y_i, A_i, X_i)$, $i = 1, \dots, n$, where $A_i \in \{0, 1\}$ is treatment, $X_i \in \mathcal{X}$ are covariates, and $Y_i = Y_i(A_i)$ under the potential outcomes framework (Imbens & Rubin 2015). Causal Bag of Little Bootstrap (Algorithm 1) partitions the indices into s disjoint subsets I_k of size b (chosen to cover almost all observations). Within each subset I_k , we fit all required objects (nuisance functions, kernel weights, and/or a decision rule) once using $\{Z_i : i \in I_k\}$, compute per-unit contributions $\{\hat{\theta}_{i,k} : i \in I_k\}$, and then generate r bootstrap replicates by multinomial reweighting of these fixed contributions; no refitting is performed within replicates.

The definition of $\hat{\theta}_{i,k}$ depends on the target. In this paper we consider inference for kernelized AOL policy learning and for the ATE:

$$\hat{\theta}_{i,k} = \begin{cases} \hat{\theta}_{i,k}^{\text{kAOL}} := \frac{|\tilde{r}_{i,k}|}{\hat{\pi}_k(A_i | X_i)} \phi\left(A_i \text{sign}(\tilde{r}_{i,k}) (\hat{h}_k(X_i) + \hat{b}_k)\right), & \text{(Section 2.1),} \\ \hat{\theta}_{i,k}^{\text{ATE}} := \hat{\psi}_{i,k}(1) - \hat{\psi}_{i,k}(0), & \text{(Sections 2.2–2.3).} \end{cases}$$

Here, for $a \in \{0, 1\}$,

$$\hat{\psi}_{i,k}(a) := \hat{m}_{a,k}(X_i) - \mathbf{1}(A_i = a) \hat{\gamma}_{a,k}(X_i) \{\hat{m}_{a,k}(X_i) - Y_i\},$$

with $(\hat{m}_{a,k}, \hat{\pi}_k, \hat{\gamma}_{a,k}, \hat{h}_k, \hat{b}_k)$ fit on I_k . In Section 2.2 (kernel minimax weights), $\hat{\gamma}_{a,k}(\cdot)$ denotes the kernel-minimax weights estimated on I_k . In Section 2.3 (DML), $\hat{\gamma}_{a,k}(X_i) = 1/\hat{\pi}_{a,k}(X_i)$, where $\hat{\pi}_{a,k}$ is the subset-trained propensity score.

This follows the same computational principle emphasized in the DML bootstrap literature: resample score/contribution terms to capture first-order uncertainty while avoiding repeated refitting of nuisance models. For example, Belloni et al. (2018) studies a multiplier bootstrap for orthogonal scores, and this approach underlies the confidence intervals implemented in the `DoubleML` package (Bach et al. 2022) for Chernozhukov et al. (2017). While this is computationally-efficient, Tang & Westling (2024) notes that not refitting the nuisance functions can lead to poor finite-sample coverage and invalid confidence intervals when certain assumptions are not satisfied. Nevertheless, we find in our simulations that nominal coverage is retained even when not refitting in each resample. This is corroborated by Theorem 1, which shows that, once the per-unit contributions have been computed on a subset, multinomial reweighting of these fixed contributions reproduces the correct large-sample sampling variability of the subset estimator, so refitting within bootstrap replicates is unnecessary for first-order coverage.

3.1 Properties

As described above, cBLB executes all expensive fitting steps (nuisance estimation, kernel-weight optimization, and/or policy learning) once per subset I_k and then holds the fitted objects fixed across the r bootstrap replicates within that subset. Our simulations show that this “no-refit within replicates” implementation attains nominal coverage in finite samples. Here we justify this choice theoretically by showing that, under standard asymptotic linearity of the corresponding full-sample estimator and mild stability of the subset-level contributions, cBLB still attains first-order (asymptotically correct) coverage despite refit-

Algorithm 1 cBLB

Require: Number of subsets s , their size b , and number of bootstrap replicates, r

for $k \leftarrow 1$ to s **do**

Randomly permute a pre-defined set of indices $\mathcal{I} = \{1, 2, \dots, n\}$ and partition into disjoint blocks $I_k = \{i_1, \dots, i_b\}$

Fit any required nuisance models and/or policy model on the subset $\{Z_i : i \in I_k\}$, and compute per-index contributions $\hat{\theta}_{i_j}$ (one value per $i_j \in I_k$), where $\hat{\theta}_{i_j}$ may depend on the fitted objects on subset k

for $\ell \leftarrow 1$ to r **do**

Sample $(M_1, \dots, M_b) \sim \text{Multinomial}(n; \frac{1}{b}, \dots, \frac{1}{b})$

Calculate the bootstrap empirical distribution $\mathbf{P}_{n,\ell}^* \leftarrow \frac{1}{n} \sum_{a=1}^b M_a \delta_{Z_{i_a}}$

Calculate the estimator as the reweighted average of the contributions: $\hat{\theta}_{n,\ell} \leftarrow \frac{1}{n} \sum_{a=1}^b M_a \hat{\theta}_{i_a}$

end for

$\text{CI}(\theta)_k \leftarrow (\hat{\theta}_k^{0.025}, \hat{\theta}_k^{0.975})$, where $\hat{\theta}_k^\alpha$ denotes the empirical α -quantile of $\{\hat{\theta}_{n,\ell}\}_{\ell=1}^r$

end for

$\text{CI}(\theta) \leftarrow \left(\frac{1}{s} \sum_{k=1}^s \hat{\theta}_k^{0.025}, \frac{1}{s} \sum_{k=1}^s \hat{\theta}_k^{0.975} \right)$

ting only at the subset level.

Theorem 1 (First-order validity of cBLB (no refit)). *Fix a subset $I_k = \{i_1, \dots, i_b\}$ of size b and fitted objects computed on $\{Z_i : i \in I_k\}$, yielding contributions $\{\hat{\theta}_{i,k} : i \in I_k\}$ and the subset estimator*

$$\hat{\theta}_k := \frac{1}{b} \sum_{i \in I_k} \hat{\theta}_{i,k}.$$

Let $M = (M_1, \dots, M_b) \sim \text{Multinomial}(n; 1/b, \dots, 1/b)$ and define the cBLB replicate

$$\hat{\theta}_{n,k}^* := \frac{1}{n} \sum_{a=1}^b M_a \hat{\theta}_{i_a,k}.$$

Assume: (i) the corresponding full-sample estimator admits an influence-function expansion with influence function $\psi \in L_2(P)$; (ii) within the fixed subset I_k , the frozen contributions satisfy the first-order approximation

$$\hat{\theta}_{i,k} = \theta_0 + \psi(Z_i) + r_{i,k}, \quad \frac{1}{\sqrt{b}} \sum_{i \in I_k} r_{i,k} = o_p(1), \quad \text{and} \quad \frac{1}{b} \sum_{i \in I_k} r_{i,k}^2 = o_p(1);$$

(iii) $b \rightarrow \infty$, $b/n \rightarrow 0$, and the partition covers all but $o(n)$ observations.

Then, conditional on $\{Z_i : i \in I_k\}$,

$$\sqrt{n}(\hat{\theta}_{n,k}^* - \hat{\theta}_k) \Rightarrow N(0, \sigma_k^2), \quad \sigma_k^2 := \text{Var}_{P_{b,k}}(\hat{\theta}_{i,k}),$$

where $P_{b,k}$ denotes the empirical distribution on $\{Z_i : i \in I_k\}$. Moreover, under (ii) and $b \rightarrow \infty$, $\frac{1}{s} \sum_{k=1}^s \sigma_k^2 \xrightarrow{p} \text{Var}\{\psi(Z)\}$ (or similarly $\forall \varepsilon > 0$, $\frac{1}{s} \sum_{k=1}^s \mathbf{1}\{|\sigma_k^2 - \text{Var}\{\psi(Z)\}| > \varepsilon\} \xrightarrow{p} 0$).

Finally, under standard BLB aggregation conditions (e.g., those ensuring that averaging subset-level bootstrap quantiles targets the corresponding quantiles of the limiting distribution), the cBLB confidence intervals produced by Algorithm 1 achieve asymptotically correct coverage for θ_0 .

Proof sketch: Theorem 1 implies that first-order coverage is governed by the estimator's leading \sqrt{n} fluctuation. Within a subset I_k , holding fitted objects fixed turns $\{\hat{\theta}_{i,k} : i \in I_k\}$ into fixed per-unit contributions and $\hat{\theta}_k = b^{-1} \sum_{i \in I_k} \hat{\theta}_{i,k}$ into their empirical mean. A cBLB replicate $\hat{\theta}_{n,k}^*$ is the mean of n draws from the empirical distribution $P_{b,k}$ on these b contributions, so conditional on $\{Z_i : i \in I_k\}$ a conditional CLT yields $\sqrt{n}(\hat{\theta}_{n,k}^* - \hat{\theta}_k) \Rightarrow N(0, \sigma_k^2)$ with $\sigma_k^2 = \text{Var}_{P_{b,k}}(\hat{\theta}_{i,k})$. Assumption (ii) implies $\sigma_k^2 \rightarrow_p \text{Var}\{\psi(Z)\}$ for a fixed subset I_k as $b \rightarrow \infty$. Since the subsets are disjoint and $s \rightarrow \infty$, a law of large numbers yields that the empirical distribution (or average) of σ_k^2 over $k = 1, \dots, s$ concentrates at $\text{Var}\{\psi(Z)\}$. Standard BLB scaling and aggregation across subsets then transfer this first-order validity to the full-sample target, yielding asymptotically correct cBLB confidence intervals for θ_0 .

Also note that Algorithm 1 uses percentile (quantile) intervals from the uncentered replicates $\{\hat{\theta}_{n,k,j}^*\}_{j=1}^r$, and Theorem 1 still applies because conditional quantiles shift by $\hat{\theta}_k$ (i.e., $Q_\alpha(\hat{\theta}_{n,k}^* | I_k) = \hat{\theta}_k + Q_\alpha(\hat{\theta}_{n,k}^* - \hat{\theta}_k | I_k)$), so first-order validity for $\hat{\theta}_{n,k}^* - \hat{\theta}_k$ implies first-order validity of the percentile CI after BLB aggregation.

For the ATE target, Theorem 1 applies because $\hat{\theta}_{i,k}^{\text{ATE}} = \hat{\psi}_{i,k}(1) - \hat{\psi}_{i,k}(0)$ is an orthogonal-score/AIPW contribution computed using objects fit on I_k . Existing results for DML and augmented minimax linear / kernel-minimax-weight estimators establish the required influence-function expansion under standard regularity and nuisance-rate conditions (Sections 2.2–2.3), which we invoke rather than re-prove.

For kernelized AOL, Theorem 1 applies to fixed-fit inference for the subset-learned scalar criterion: within each subset I_k we learn (\hat{h}_k, \hat{b}_k) (and any nuisance components entering $\tilde{r}_{i,k}$ and $\hat{\pi}_k$) once, then treat these fitted objects as fixed and bootstrap

$$\hat{\theta}_k^{\text{kAOL}} = \frac{1}{b} \sum_{i \in I_k} \hat{\theta}_{i,k}^{\text{kAOL}}$$

by multinomial reweighting of $\{\hat{\theta}_{i,k}^{\text{kAOL}} : i \in I_k\}$. Conditional on the subset-fitted objects, this is an empirical mean of i.i.d. terms, so the cBLB step provides a first-order valid approximation for this fixed-fit criterion. Consequently, in applied use, the cBLB confidence interval for kernelized AOL quantifies first-order sampling uncertainty for the estimated value/criterion of the specific rule trained and then held fixed (within each subset), and it should not be read as uncertainty about the learned rule itself or the optimal value after re-optimizing.

Theorem 1 does *not* address inference for the sampling distribution of the learned decision rule itself (e.g., (\hat{h}_k, \hat{b}_k)), nor the value of a rule re-optimized within each bootstrap replicate, nor “optimal value” statements involving an $\arg \min / \arg \max$ over a function class; these require separate analysis.

3.1.1 Computational complexity

Let $C_{\text{fit}}(m)$ be the cost of running the full fitting pipeline (nuisance fits and any kernel-weight/policy optimization) on m observations. A standard bootstrap with r refits costs

$$T_{\text{boot}} = \Theta(r C_{\text{fit}}(n)).$$

cBLB fits once per subset and only reweights within replicates, so

$$T_{\text{cBLB}} = \Theta(s C_{\text{fit}}(b)) + \Theta(srb).$$

With disjoint subsets covering most observations ($s \asymp n/b$),

$$T_{\text{cBLB}} = \Theta\left(\frac{n}{b} C_{\text{fit}}(b)\right) + \Theta(nr).$$

Thus, when $C_{\text{fit}}(m)$ grows faster than linearly in m (typical for kernel methods/convex programs), taking $b = n^\gamma$ with $\gamma \in (0, 1)$ yields a strict asymptotic improvement over T_{boot} .

4 Simulation

We conduct three simulations considering three estimators: AOL for policy learning, and kernel minimax weights, and DML for estimation of causal effects.

Data-generating mechanism: For policy learning, the DGP comes from Zhou & Kosorok (2017) and is shown in (1).

$$\begin{aligned}
 X_1, X_2, \dots, X_5 &\stackrel{\text{i.i.d.}}{\sim} \text{Unif}(-1, 1) \\
 \Pr(W = 1|\mathbf{X}) &= \Pr(W = -1|\mathbf{X}) = 0.5 \\
 \epsilon &\sim \text{Normal}(0, 1) \\
 Y &= 0.5 + 0.5X_1 + 0.8X_2 + 0.3X_3 - 0.5X_4 + 0.7X_5 + \\
 &\quad + W(0.2 - 0.6X_1 - 0.8X_2) + \epsilon
 \end{aligned} \tag{1}$$

In this case, the optimal policy is given by:

$$\delta(\mathbf{X}) = \begin{cases} 1 & 0.2 - 0.6X_1 - 0.8X_2 > 0 \\ 0 & \text{otherwise} \end{cases}$$

For for estimation of causal effects with kernel minimax weights and DML, the data-generating process (DGP) is delineated in equation (2).

$$\begin{aligned}
 X_1, X_2 &\stackrel{\text{i.i.d.}}{\sim} \text{Normal}(0, 1) \\
 \Pr(W = 1|X_1, X_2) &= \frac{1}{1 + \exp(-0.5X_1 - 0.5X_2)} \\
 \epsilon &\sim \text{Normal}(0, 1) \\
 Y(0) &= X_1 + X_2 + \epsilon \\
 Y(1) &= Y(0) + \tau W.
 \end{aligned} \tag{2}$$

For each individual subject i , we generate two independent confounding variables (X_{1i}, X_{2i}) and calculate the propensity score by applying the inverse-logit function to a linear amalgamation of these covariates. An error term ϵ is then drawn independently and identically from a standard normal distribution to construct the outcomes under control and treatment conditions. The treatment effect remains constant across all subjects, with $\tau = 0.8$. The level of overlap between covariates is regulated by a specific parameter in the inverse-logit equation; a value of $-\frac{1}{2}$ is used to create a certain degree of imbalance between the treatment and control groups in relation to some of the covariates.

Estimand: For the optimal policy case, the estimand is the optimal value, that is, the expected outcome when the optimal policy is followed. For DML and kernel minimax weights, the estimand of interest τ is the average treatment effect (ATE): $\tau = E(Y(1) - Y(0))$.

Methods: We construct 1000 replications of the DGP varying the number of subsets s .

For policy learning, we estimate individualized treatment regimes by solving a regularized empirical risk minimization problem using an augmented outcome-weighted learning (AOL) loss function:

$$\min_f \frac{1}{n} \sum_{i=1}^n \frac{|\tilde{r}_i|}{\pi(w_i, \mathbf{x}_i)} \phi(a_i \text{sign}(\tilde{r}_i f(\mathbf{x}_i))) + \frac{\lambda}{2} \|f\|^2$$

where f is the non-linear decision boundary (represented by $h(\mathbf{x}) + b$ with $h(\mathbf{x}) \in \mathcal{H}_K$, a reproducing kernel Hilbert space associated with the linear kernel function K), \tilde{r}_i is a residual of a regression of the outcome on a function of covariates, $\|f\|$ is the norm $\|\cdot\|_K$, ϕ is the Huberized hinge loss function, and λ is a tuning parameter.

For DML, both the outcome and propensity score models are fit using SVM with a linear kernel. For kernel minimax weights, as proposed previously (Kallus et al. 2021, Kallus &

Santacatterina 2022), we used a polynomial kernel $\mathcal{K}_a(z, z') = C(z^\top z')^{d_1} + \sigma_a^2 \delta^*(z, z')$, fixing $d_1 = 1$ and tuning C and σ_a^2 as hyperparameters; for data generation/modeling we assumed the arm-specific regression functions $m_1(X)$ and $m_0(X)$ follow Gaussian process priors with kernels \mathcal{K}_1 and \mathcal{K}_0 , and outcomes satisfy $Y_i = m(Z_i) + \varepsilon_i$ with $\varepsilon_i \sim \mathcal{N}(0, \sigma_a^2)$.

Performance Measures: We construct percentile confidence intervals (Efron & Tibshirani 1994). We want to ensure that the bootstrapped confidence intervals have at least nominal coverage, i.e.,

$$\Pr(\tau \in \text{CI}^*) \geq 1 - \alpha.$$

Full Sample Timing Comparison To show the timing advantages of the cBLB, we compare the timing of the cBLB to a fair comparison of the full-sample bootstrap, where we do not re-fit or re-optimize in each bootstrap resample. All optimization/fitting is done once.

4.1 Results

Coverage Figures 1, 3, and 2 show “zip plots” of the confidence intervals for varying s (Morris et al. 2019). We see that we are able to obtain nominal coverage in each case (although DML is slightly conservative).

Timing.

Figures 4, 5, and 6 show the comparison of the full bootstrap analogue to our cBLB for 25 replications.¹ In addition, figure 7 shows how poorly full bootstrap scales for large data in the policy learning case.

¹The full bootstrap here mimics cBLB in not refitting within each bootstrap resample.

Kernelized AOL, optimal value $n = 5000$

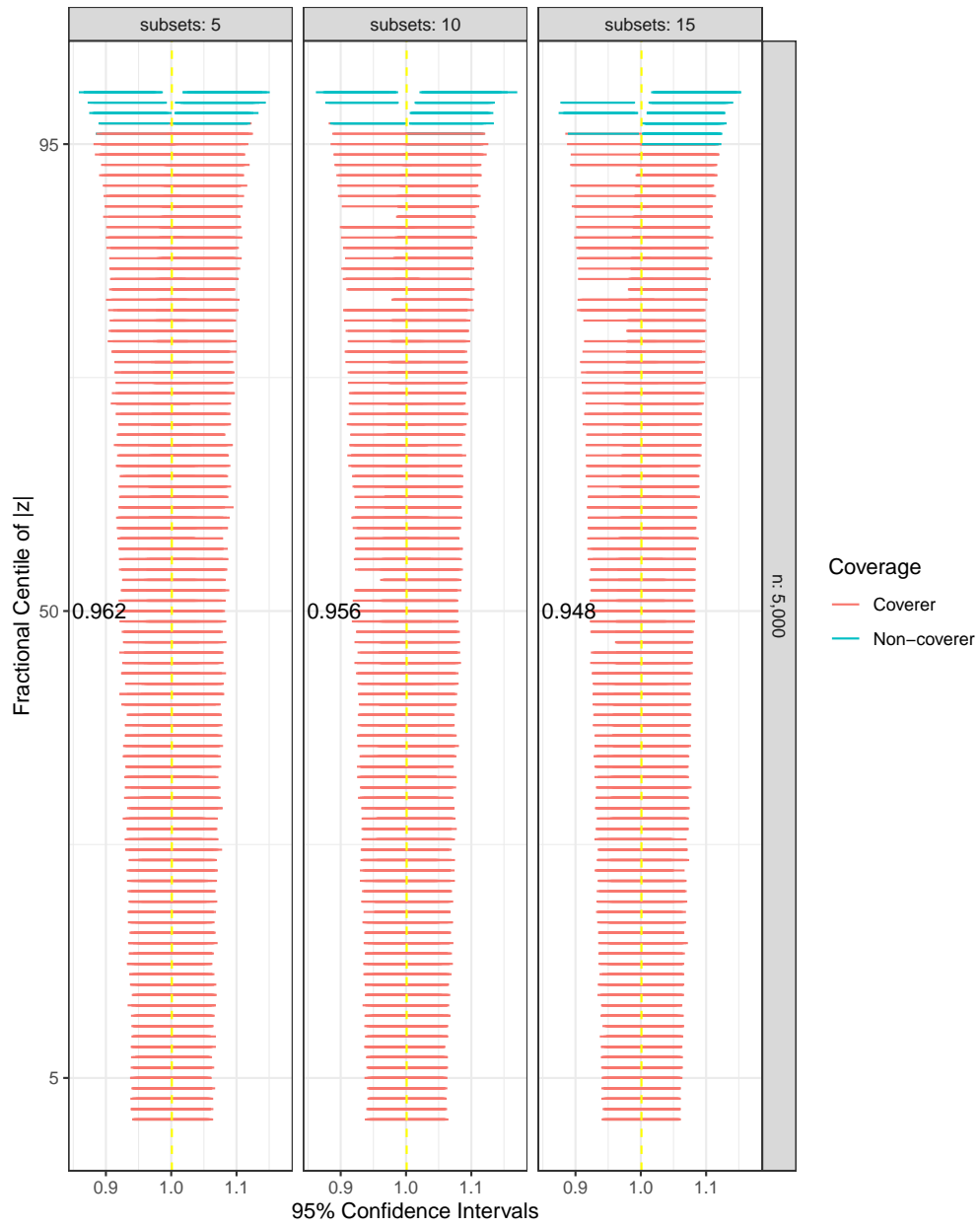


Figure 1: Confidence intervals for the optimal value from 1000 replications from the cBLB algorithm, Kernelized AOL)

Kernel Minimax Weights n = 5000

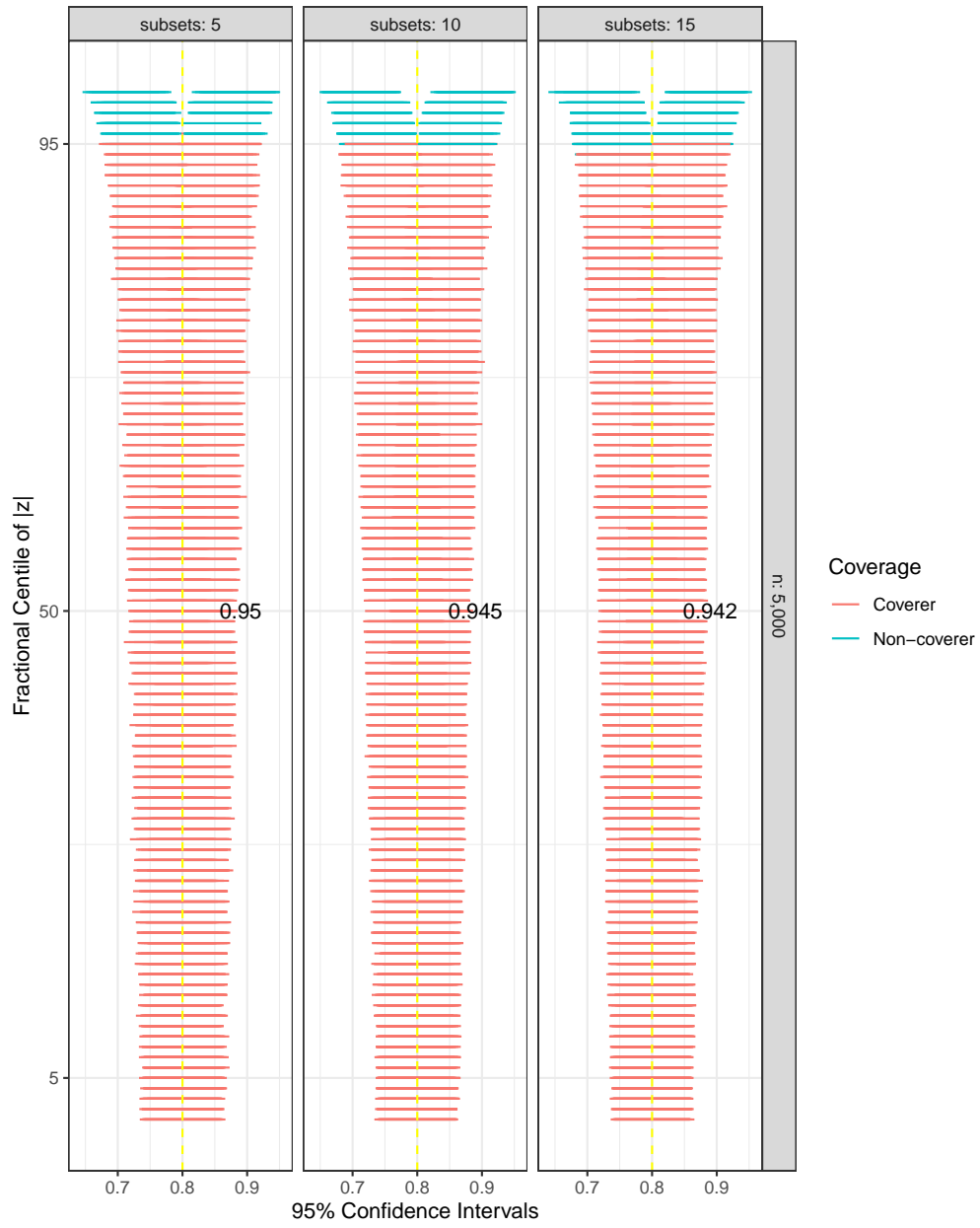


Figure 2: Confidence intervals for the ATE from 1000 replications from the cBLB algorithm, Kernel Minimax Weights)

DML using SVM and cross-fitting $n = 5000$

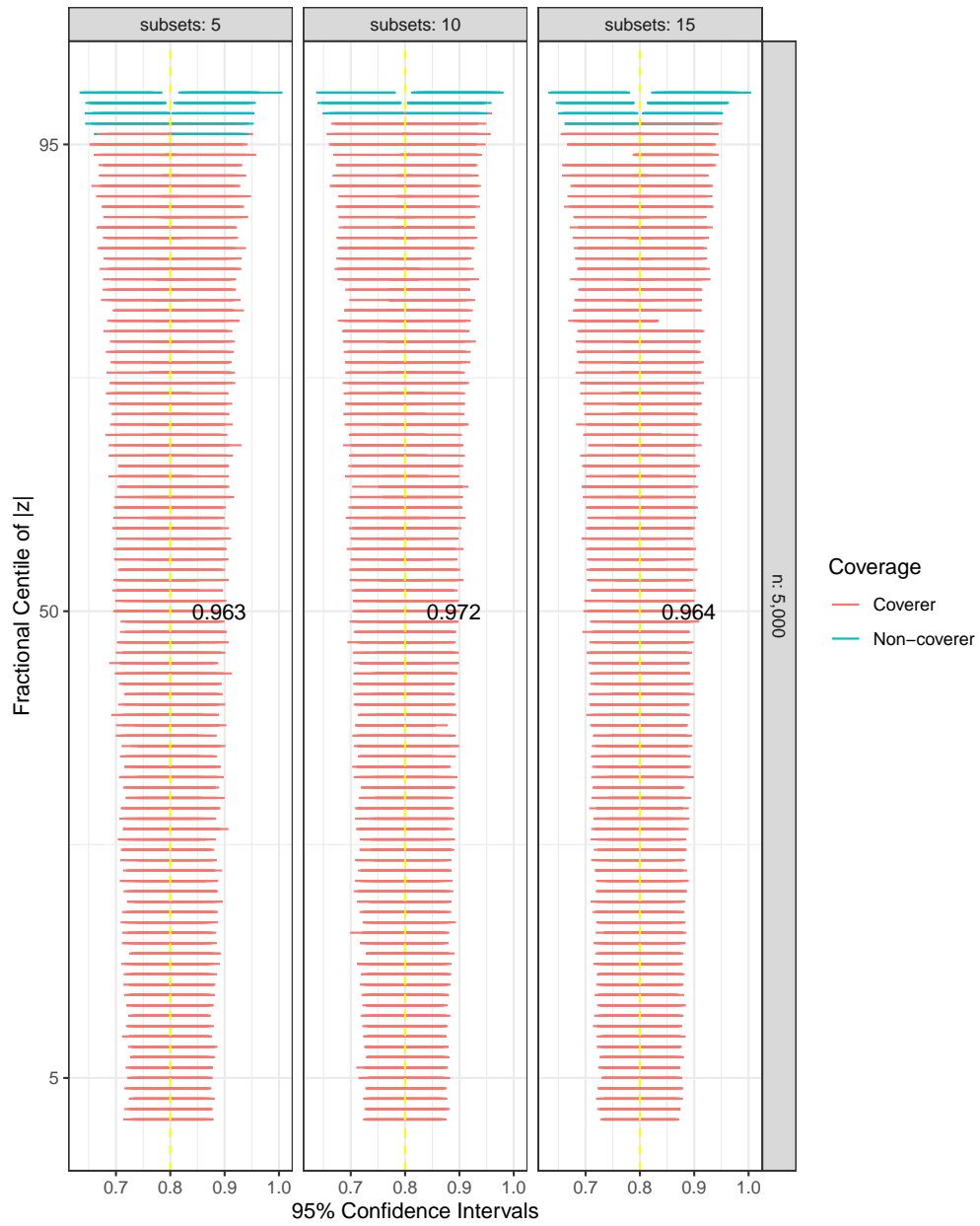


Figure 3: Confidence intervals for the ATE from 1000 replications from the cBLB algorithm, DML using SVM and cross-fitting)

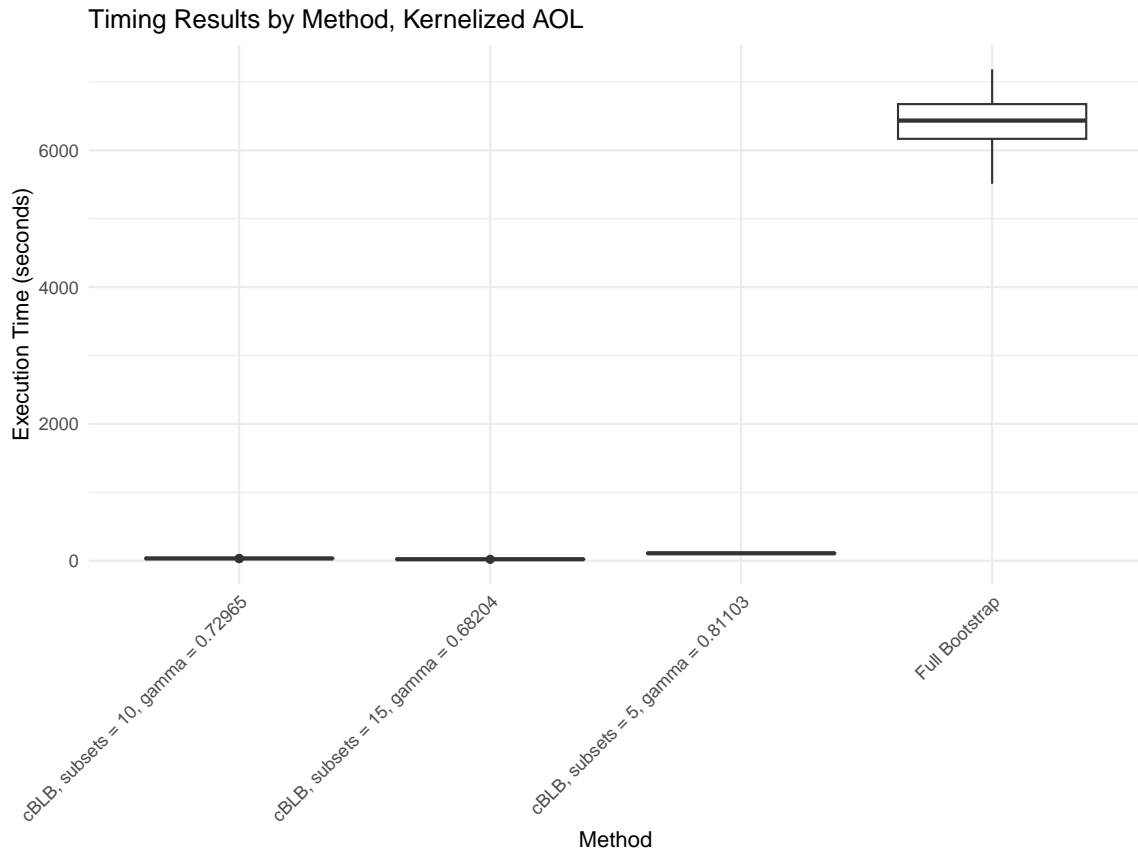


Figure 4: Timing results from 25 replications of the cBLB algorithm ($n = 5000$) for Kernelized AOL

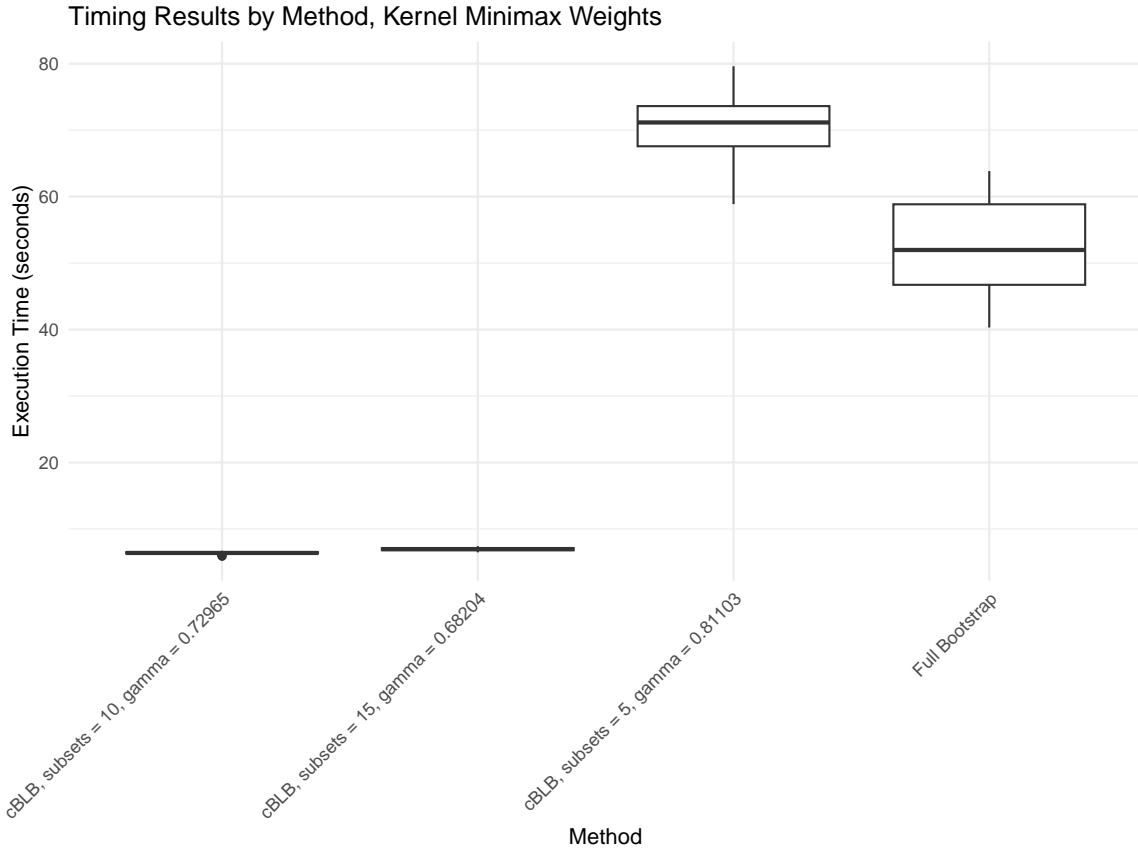


Figure 5: Timing results from 25 replications of the cBLB algorithm ($n = 5000$) for Kernel Minimax Weights

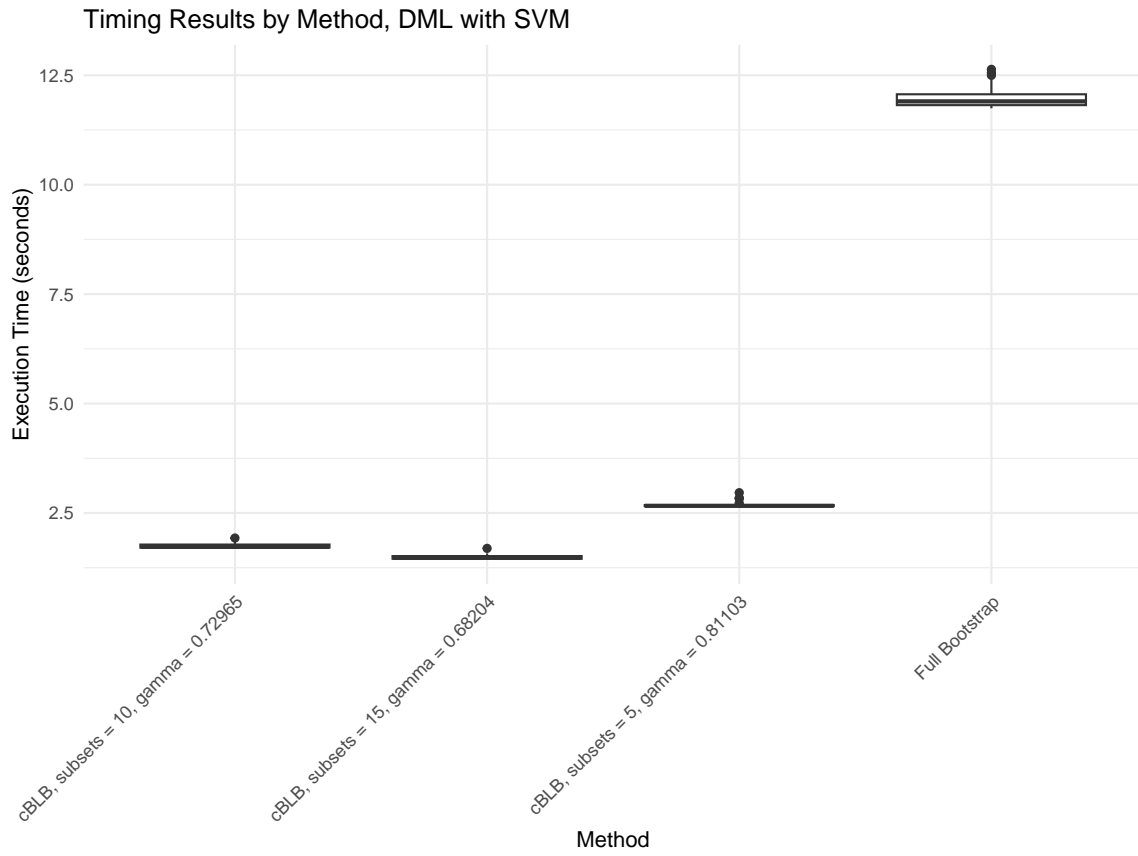


Figure 6: Timing results from 25 replications of the cBLB algorithm ($n = 5000$) for DML with SVM

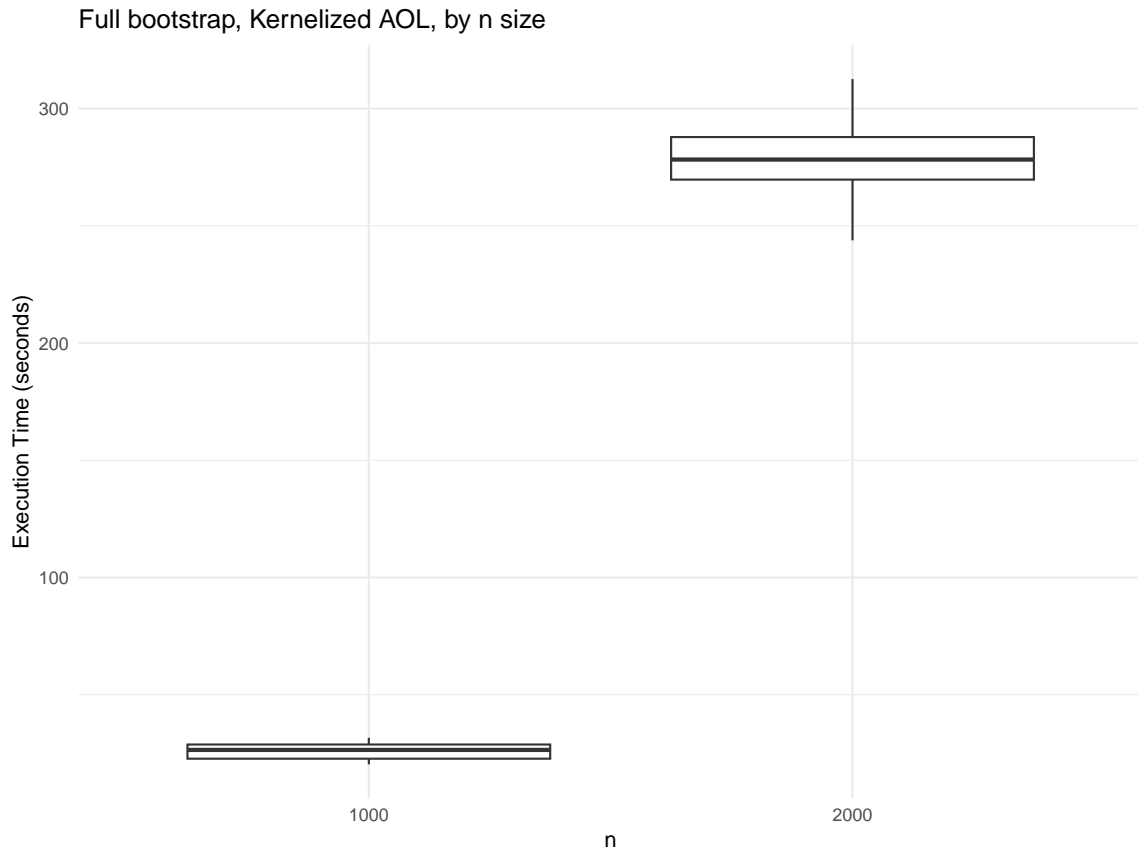


Figure 7: Timing results from 25 replications of the full bootstrap for policy learning with Kernelized AOL

4.2 Practical Considerations

4.2.1 Size of the subsets b

The selection of subset size and the number of such subsets are closely interrelated and influence one other. Generally, a smaller number of observations within each subset necessitates a greater number of subsets to yield satisfactory results. In the foundational BLB paper, the authors recommend a formula for determining subset sizes b relying on a parameter γ such that $b = n^\gamma$ (Kleiner et al. 2014, p. 20). After extensive simulations, they conclude that a γ value of 0.7 often serves as "an effective and sensible choice" in a variety of contexts (Kleiner et al. 2014, p. 20). In our previous work Kosko et al. (2024), we found that the appropriate γ changes by estimating method. In this paper, we recommend deciding on the subset size based on domain knowledge, trading off the computational complexity of the algorithm against the minimum number of observations needed to accurately optimize or estimate. Each subset size was chosen to be in the several hundreds or low thousands of observations.

4.2.2 Number of subsets s

The number of subsets required depends on the size of the subset chosen. In the original paper, Kleiner et al. (2014) found that 1-2 subsets could be sufficient for a $\gamma = 0.9$ and recommended 10-20 subsets for $\gamma = 0.7$. Kleiner et al. (2014) prove that the BLB enjoys the same higher order correctness as the bootstrap as long as we choose disjoint subsets and the number of subsets is approximately $\frac{n}{b}$. Thus, once the subset size or number of subsets is decided, the other is given automatically by the formula $b \approx \frac{n}{s}$.

4.2.3 Estimands

Our simulations estimate (1) the ATE and (2) the optimal value of an outcome from the optimal regime, but we can in fact calculate any type of estimand with the cBLB. It is agnostic to estimand.

4.2.4 Constructing confidence intervals and hypothesis tests

We can use any method to construct confidence intervals, including percentile and normal (Efron & Tibshirani 1994, Davison & Hinkley 1997). In this simulation, we use percentile.

5 Application to the 2023 U.S. Natality Data

5.1 Study Population

We conducted a case study using the 2023 U.S. natality public-use microdata 2023 Natality Public Use File from the National Vital Statistics System (NVSS), compiled by the National Center for Health Statistics (NCHS) from U.S. birth certificates submitted by state and territorial vital registration jurisdictions (National Center for Health Statistics 2024).

The 2023 data contains 3,605,081 U.S. birth records (National Center for Health Statistics 2024). NCHS reports that more than 99% of births occurring in the United States in 2023 were registered, and emphasizes that item-level completeness varies across variables and jurisdictions (National Center for Health Statistics 2024).

The dataset includes detailed measures of maternal sociodemographic characteristics (e.g., age, race/ethnicity, education, marital status), paternal characteristics, prenatal care utilization (e.g., month prenatal care began, number of visits), maternal behaviors and health (e.g., cigarette use before and during pregnancy, pre-pregnancy BMI), labor/delivery

Table 1: Baseline characteristics by smoking status (NVSS)

Smoking status	N	Mean birthweight	SD birthweight	Mean age	SD age
Non-smoker	2,882,907	3279.397	552.137	29.401	5.797
Smoker	97,832	3056.878	589.699	29.277	5.623

characteristics, and infant outcomes(National Center for Health Statistics 2024).

The analytic cohort was restricted to singleton live births with plausible birthweights (350–6000 g) and complete information on maternal and pregnancy covariates. The primary outcome was infant birthweight in grams, and the exposure was an indicator for any maternal cigarette use during pregnancy, defined as positive self-reported cigarettes per day in any trimester. To address confounding, we adjusted for maternal age, education, race, Hispanic origin, marital status, parity, prenatal care timing, and payment source. We learned an individualized treatment regime using Kernelized Augmented Outcome-Weighted Learning and then estimated the value of the learned regime. We estimated ATE using both Kernel Minimax Weights with kernels as in our simulations and DML with a linear kernel.

Table 1 shows some baseline characteristics of the sample by smoking status. Table 2 shows the distribution of important covariates by smoking status.

5.2 Results

Table 3 presents the causal estimates, confidence intervals, and computation times for each method using the cBLB procedure. We organize our discussion around three aspects: the substantive estimates, their alignment with the existing literature, and the computational

performance of the cBLB relative to the standard bootstrap.

5.2.1 Average treatment effect estimates

The kernel minimax weights estimator yields an estimated ATE of -217.1 grams (95% CI: $-220.9, -213.2$), while the DML with SVM estimator produces an estimate of -185.8 grams (95% CI: $-189.9, -181.7$). Both estimates are negative, statistically significant, and fall within the range of 150–250 grams typically reported in the epidemiological literature on smoking and birthweight (Hellerstedt et al. 1997, Wisborg et al. 2001, Cattaneo 2010). The confidence intervals are narrow, reflecting the precision afforded by the large sample size, with standard errors of 1.86 and 2.03 grams, respectively. The approximately 31-gram discrepancy between the two ATE estimates likely reflects differences in the underlying modeling assumptions: the kernel minimax approach minimizes worst-case covariate imbalance in a reproducing kernel Hilbert space, while the DML estimator relies on SVM-based nuisance function estimation with cross-fitting. Despite this difference, the qualitative conclusions are consistent across both methods.

5.2.2 Optimal regime value

The kernelized AOL estimator yields an estimated optimal value of 3,253.6 grams (95% CI: 3,250.0, 3,257.2). This quantity is on a fundamentally different scale from the ATE estimates: it represents the expected birthweight when each mother is assigned to the treatment recommended by the learned optimal regime. Given the well-established harm of smoking, the learned regime effectively recommends abstinence from smoking for all mothers, and the estimated optimal value is therefore interpretable as the mean birthweight in a population where no mother smokes during pregnancy. This estimate is consistent with population-level mean birthweights reported for nonsmoking mothers in the United States

(National Center for Health Statistics 2024), and it aligns with our estimated mean birth-weight had everyone not smoked from DML with SVM and AMLE (point estimates 3,278.1 and 3,278.5, respectively; Table 3). Together, these results support that the learned policy is optimal in this setting, namely, recommending that no one smoke during pregnancy. As discussed in Section 3.1, the cBLB confidence interval for kernelized AOL quantifies first-order sampling uncertainty for the estimated value/criterion of the specific rule trained and then held fixed (within each subset), and it should not be read as uncertainty about the learned rule itself or the optimal value after re-optimizing.

5.2.3 Computational performance

A central motivation for this work is the computational infeasibility of standard bootstrap inference with kernel-based estimators at this scale. In our application, the standard non-parametric bootstrap failed outright for both the kernel minimax weights and kernelized AOL estimators, and ran for approximately one week without producing results for the DML estimator. By contrast, the cBLB procedure successfully produced valid confidence intervals for all three methods, with computation times ranging from approximately 5.7 hours for kernel minimax weights to 10.9 hours for DML with SVM and 96.5 hours for kernelized AOL. The longer runtime for kernelized AOL reflects the $\mathcal{O}(n^2)$ cost of computing and manipulating the kernel Gram matrix within each subset, compounded by the L-BFGS optimization required for policy learning. These computation times were obtained without parallelization across subsets; exploiting the embarrassingly parallel structure of cBLB would reduce runtimes proportionally to the number of available cores.

6 Conclusions

This paper addresses the pressing computational challenges of conducting valid inference with kernel-based causal estimators on large real-world datasets. Building on recent work on the causal bag of little bootstraps (cBLB), we extend this scalable bootstrap framework to accommodate a wide class of kernel-based methods used in causal inference. These include kernel minimax weights in reproducing kernel Hilbert spaces (RKHS), doubly robust estimators within the double machine learning (DML) framework, and optimal policy learning estimators based on residual weighted classification.

Through extensive simulations, we demonstrate that the proposed algorithm achieves nominal coverage for confidence intervals while offering dramatic improvements in computational efficiency compared to standard nonparametric bootstrapping. These gains hold across a range of causal estimands, including average treatment effects and optimal policy values, and across multiple domains with varying levels of model complexity. The results also suggest that cBLB can deliver reliable inference even when nuisance components are estimated using complex machine learning models.

From a methodological standpoint, our work contributes a flexible resampling framework that is agnostic to the causal estimand and can be adapted to other high-dimensional or kernel-based methods, including those based on Gaussian processes, support vector machines, and RKHS-regularized estimators. This flexibility is crucial for practitioners seeking scalable uncertainty quantification tools that maintain statistical rigor in the presence of rich covariate information and complex treatment assignment mechanisms.

However, several limitations remain. First, although our method avoids repeated nuisance model fitting in the bootstrap loop, this relies on the assumption that re-using fitted nuisance functions provides adequate finite-sample inference. While our simulations and

theory suggest this is reasonable in practice, there may be situations in which this assumption may fail. Second, the performance of our algorithm depends on subset size and the number of bags, which require tuning and may depend on the data generating process or estimand. Third, the current implementation does not include automatic selection of kernel parameters or regularization penalties, which may limit performance in some applications. Fourth, in this paper, we do not provide theoretical guarantees for (i) the distribution of the learned decision rule itself, (ii) the value of a re-learned rule obtained by re-optimizing the policy objective inside each bootstrap replicate, or (iii) “optimal value” targets defined by maximization over a rich policy class; these problems can be nonregular and generally require separate stability/smoothness arguments beyond the fixed-fit resampling results above. These questions are left for future work.

Future research should explore adaptive schemes for choosing hyperparameters within the cBLB, including automated tuning of subset size, kernel bandwidths, and regularization parameters. Additionally, further theoretical work is needed to characterize the finite-sample coverage properties of BLB-style methods. Lastly, extending the cBLB to multi-valued or continuous treatment settings and time-varying exposures would further increase its practical relevance, especially in biomedical and policy evaluation contexts.

Overall, our results show that scalable inference for kernel-based causal estimators is not only feasible but also statistically valid in a wide range of realistic scenarios. We believe that the proposed approach provides a valuable blueprint for integrating advanced machine learning estimators into causal analysis pipelines at scale.

References

- Abadie, A. & Imbens, G. W. (2008), ‘On the failure of the bootstrap for matching estimators’, *Econometrica* **76**(6), 1537–1557.
- Abadie, A. & Spiess, J. (2022), ‘Robust post-matching inference’, *Journal of the American Statistical Association* **117**(538), 983–995.
- Adegboye, A. R., Rossner, S., Neovius, M., Lourenço, P. M. & Linné, Y. (2010), ‘Relationships between prenatal smoking cessation, gestational weight gain and maternal lifestyle characteristics’, *Women and Birth* **23**(4), 129–35.
- Adusumilli, K. (2018), Bootstrap inference for propensity score matching, Technical report, Working paper.
- Bach, P., Chernozhukov, V., Kurz, M. S. & Spindler, M. (2022), ‘Doubleml—an object-oriented implementation of double machine learning in python’, *Journal of Machine Learning Research* **23**(53), 1–6.
- Bargagli-Stoffi, F. J., Cadei, R., Lee, K. & Dominici, F. (2020), ‘Causal rule ensemble: Interpretable discovery and inference of heterogeneous treatment effects’, *arXiv preprint arXiv:2009.09036* .
- Belloni, A., Chernozhukov, V., Chetverikov, D. & Wei, Y. (2018), ‘Uniformly valid post-regularization confidence regions for many functional parameters in z-estimation framework’, *Annals of statistics* **46**(6B), 3643.
- Ben-Michael, E., Feller, A., Hirshberg, D. A. & Zubizarreta, J. R. (2021), ‘The balancing act in causal inference’, *arXiv preprint arXiv:2110.14831* .

- Cattaneo, M. D. (2010), ‘Efficient semiparametric estimation of multi-valued treatment effects under ignorability’, *Journal of econometrics* **155**(2), 138–154.
- Chapelle, O. (2007), ‘Training a support vector machine in the primal’, *Neural computation* **19**(5), 1155–1178.
- Chernozhukov, V., Chetverikov, D., Demirer, M., Duflo, E., Hansen, C. & Newey, W. (2017), ‘Double/debiased/neyman machine learning of treatment effects’, *American Economic Review* **107**(5), 261–65.
- Colangelo, K. & Lee, Y.-Y. (2020), ‘Double debiased machine learning nonparametric inference with continuous treatments’, *arXiv preprint arXiv:2004.03036* .
- Dagan, N., Barda, N., Kepten, E., Miron, O., Perchik, S., Katz, M. A., Hernán, M. A., Lipsitch, M., Reis, B. & Balicer, R. D. (2021), ‘Bnt162b2 mrna covid-19 vaccine in a nationwide mass vaccination setting’, *New England Journal of Medicine* .
- Davison, A. C. & Hinkley, D. V. (1997), *Bootstrap methods and their application*, number 1, Cambridge university press.
- de Bont, J., Krishna, B., Stafoggia, M., Banerjee, T., Dholakia, H., Garg, A., Ingole, V., Jaganathan, S., Kloog, I., Lane, K. et al. (2024), ‘Ambient air pollution and daily mortality in ten cities of india: a causal modelling study’, *The Lancet Planetary Health* **8**(7), e433–e440.
- Efron, B. (1979), ‘Bootstrap methods: another look at the jackknife’, *The Annals of Statistics* **7**, 1–26.
- Efron, B. & Tibshirani, R. J. (1994), *An introduction to the bootstrap*, CRC press.

- Fu, S., He, Q., Zhang, S. & Liu, Y. (2019), ‘Robust outcome weighted learning for optimal individualized treatment rules’, *Journal of biopharmaceutical statistics* **29**(4), 606–624.
- Hellerstedt, W. L., Himes, J. H., Story, M., Alton, I. R. & Edwards, L. E. (1997), ‘The effects of cigarette smoking and gestational weight change on birth outcomes in obese and normal-weight women’, *American Journal of Public Health* **87**(4), 591–6.
- Hirshberg, D. A. & Wager, S. (2021), ‘Augmented minimax linear estimation’, *The Annals of Statistics* **49**(6), 3206–3227.
- Imai, K. & Ratkovic, M. (2013), ‘Estimating treatment effect heterogeneity in randomized program evaluation’, *Annals of Applied Statistics* **7**(1), 443–470.
- Imai, K. & Ratkovic, M. (2014), ‘Covariate balancing propensity score’, *Journal of the Royal Statistical Society: Series B (Statistical Methodology)* **76**(1), 243–263.
- Imbens, G. W. & Rubin, D. B. (2015), *Causal inference in statistics, social, and biomedical sciences*, Cambridge University Press.
- Kallus, N. (2020), ‘Generalized optimal matching methods for causal inference’, *Journal of Machine Learning Research* **21**(62), 1–54.
- Kallus, N., Pennicooke, B. & Santacatterina, M. (2021), ‘More robust estimation of average treatment effects using kernel optimal matching in an observational study of spine surgical interventions’, *Statistics in medicine* **40**(10), 2305–2320.
- Kallus, N. & Santacatterina, M. (2019), ‘Kernel optimal orthogonality weighting: A balancing approach to estimating effects of continuous treatments’, *arXiv preprint arXiv:1910.11972* .

- Kallus, N. & Santacatterina, M. (2022), ‘Optimal weighting for estimating generalized average treatment effects’, *Journal of Causal Inference* **10**(1), 123–140.
- Kang, J. D. & Schafer, J. L. (2007), ‘Demystifying double robustness: A comparison of alternative strategies for estimating a population mean from incomplete data’.
- Kennedy, E. H. (2022), ‘Semiparametric doubly robust targeted double machine learning: a review’, *arXiv preprint arXiv:2203.06469* .
- Kennedy, E. H. (2023), ‘Towards optimal doubly robust estimation of heterogeneous causal effects’, *Electronic Journal of Statistics* **17**(2), 3008–3049.
- Kennedy, E. H., Ma, Z., McHugh, M. D. & Small, D. S. (2017), ‘Non-parametric methods for doubly robust estimation of continuous treatment effects’, *Journal of the Royal Statistical Society Series B: Statistical Methodology* **79**(4), 1229–1245.
- Kim, K., Niknam, B. A. & Zubizarreta, J. R. (2023), ‘Scalable kernel balancing weights in a nationwide observational study of hospital profit status and heart attack outcomes’, *Biostatistics* p. kxad032.
- Kleiner, A., Talwalkar, A., Sarkar, P. & Jordan, M. I. (2014), ‘A scalable bootstrap for massive data’, *Journal of the Royal Statistical Society: Series B (Statistical Methodology)* **76**(4), 795–816.
- Kosko, M., Wang, L. & Santacatterina, M. (2024), ‘A fast bootstrap algorithm for causal inference with large data’, *Statistics in Medicine* **43**(15), 2894–2927.
- Morris, T. P., White, I. R. & Crowther, M. J. (2019), ‘Using simulation studies to evaluate statistical methods’, *Statistics in medicine* **38**(11), 2074–2102.

Naimi, A. I. & Kennedy, E. H. (2017), ‘Nonparametric double robustness’, *arXiv preprint arXiv:1711.07137* **476**.

Naimi, A. I., Mishler, A. E. & Kennedy, E. H. (2023), ‘Challenges in obtaining valid causal effect estimates with machine learning algorithms’, *American Journal of Epidemiology* **192**(9), 1536–1544.

National Center for Health Statistics (2024), ‘User guide to the 2023 natality public use file’, PDF documentation. Accessed 2026-02-17.

URL: https://ftp.cdc.gov/pub/health_statistics/nchs/dataset_documentation/DVS/natality/UserGuide2

Nazaret, A. & Sapiro, G. (2023), ‘A large-scale observational study of the causal effects of a behavioral health nudge’, *Science Advances* **9**(38), eadi1752.

Otsu, T. & Rai, Y. (2017), ‘Bootstrap inference of matching estimators for average treatment effects’, *Journal of the American Statistical Association* **112**(520), 1720–1732.

Pedregosa, F., Varoquaux, G., Gramfort, A., Michel, V., Thirion, B., Grisel, O., Blondel, M., Prettenhofer, P., Weiss, R., Dubourg, V., Vanderplas, J., Passos, A., Cournapeau, D., Brucher, M., Perrot, M. & Duchesnay, E. (2011), ‘Scikit-learn: Machine learning in Python’, *Journal of Machine Learning Research* **12**, 2825–2830.

Robins, J., Li, L., Tchetgen, E., van der Vaart, A. et al. (2008), Higher order influence functions and minimax estimation of nonlinear functionals, *in* ‘Probability and statistics: essays in honor of David A. Freedman’, Vol. 2, Institute of Mathematical Statistics, pp. 335–422.

Rotnitzky, A., Smucler, E. & Robins, J. M. (2021), ‘Characterization of parameters with a mixed bias property’, *Biometrika* **108**(1), 231–238.

- Santacatterina, M. & Kallus, N. (2021), ‘Optimal balancing of time-dependent confounders for marginal structural models’, *Journal of Causal Inference* **9**(1), 345–369.
- Singh, R., Xu, L. & Gretton, A. (2024), ‘Kernel methods for causal functions: dose, heterogeneous and incremental response curves’, *Biometrika* **111**(2), 497–516.
- Tang, Z. & Westling, T. (2024), ‘Consistency of the bootstrap for asymptotically linear estimators based on machine learning’, *arXiv preprint arXiv:2404.03064* .
- Wisborg, K., Henriksen, T. B., Hedegaard, M. & Secher, N. J. (2001), ‘Maternal smoking and gestational age in twin pregnancies’, *Acta Obstetrica et Gynecologica Scandinavica* **80**(10), 917–921.
- Wu, X., Mealli, F., Kioumourtzoglou, M.-A., Dominici, F. & Braun, D. (2024), ‘Matching on generalized propensity scores with continuous exposures’, *Journal of the American Statistical Association* **119**(545), 757–772.
- Zhang, Y. & Sabbaghi, A. (2021), ‘The designed bootstrap for causal inference in big observational data’, *Journal of Statistical Theory and Practice* **15**(4), 1–26.
- Zhao, Q., Small, D. S. & Bhattacharya, B. B. (2019), ‘Sensitivity analysis for inverse probability weighting estimators via the percentile bootstrap’, *Journal of the Royal Statistical Society: Series B (Statistical Methodology)* **81**(4), 735–761.
- Zhao, Y., Zeng, D., Rush, A. J. & Kosorok, M. R. (2012), ‘Estimating individualized treatment rules using outcome weighted learning’, *Journal of the American Statistical Association* **107**(499), 1106–1118.
- Zhou, X. & Kosorok, M. R. (2017), ‘Augmented outcome-weighted learning for optimal treatment regimes’, *arXiv preprint arXiv:1711.10654* .

Zhou, X., Mayer-Hamblett, N., Khan, U. & Kosorok, M. R. (2017), ‘Residual weighted learning for estimating individualized treatment rules’, *Journal of the American Statistical Association* **112**(517), 169–187.

Table 2: Covariate distributions by smoking status (NVSS)

Covariate	Level	Non-smoker	Smoker
Age-group	< 20	120,609 (4.2%)	2,955 (3.0%)
	20-24	510,662 (17.7%)	19,070 (19.5%)
	25-29	805,023 (27.9%)	28,421 (29.1%)
	30-34	872,505 (30.3%)	28,933 (29.6%)
	35-39	464,653 (16.1%)	14,940 (15.3%)
	40+	109,455 (3.8%)	3,513 (3.6%)
Education	8th grade or less	97,117 (3.4%)	2,035 (2.1%)
	9th through 12th grade with no diploma	218,887 (7.6%)	21,702 (22.2%)
	Associate degree (AA, AS)	246,091 (8.5%)	5,256 (5.4%)
	Bachelor's degree (BA, AB, BS)	661,003 (22.9%)	2,674 (2.7%)
	Doctorate (PhD, EdD) or Professional Degree (MD, DDS, DVM, LLB, JD)	91,746 (3.2%)	79 (0.1%)
	High school graduate or GED completed	764,892 (26.5%)	44,812 (45.8%)
	Master's degree (MA, MS, MEng, MEd, MSW, MBA)	312,907 (10.9%)	542 (0.6%)
	Some college credit, but not a degree	490,264 (17.0%)	20,732 (21.2%)
Precare	No prenatal care	63,948 (2.2%)	6,631 (6.8%)
Race	AIAN (only)	28,036 (1.0%)	2,323 (2.4%)
	Asian (only)	155,581 (5.4%)	392 (0.4%)
	Black (only)	475,092 (16.5%)	12,599 (12.9%)
	More than one race	80,133 (2.8%)	4,486 (4.6%)
	NHOPI (only)	10,863 (0.4%)	173 (0.2%)
	White (only)	2,133,202 (74.0%)	77,859 (79.6%)

Table 3: ATE estimates and mean outcome under the optimal policy for the NVSS dataset

Setting	$E(Y(0))^a$	Lower CI	Upper CI	Estim.	S.E.	Time (seconds)
Kernel minimax weights	3278.498	-220.854	-213.237	-217.051	1.863	20506.980
DML with SVM	3278.142	-189.923	-181.682	-185.838	2.031	39260.148
Kernelized AOL	–	3249.961	3257.212	3253.579	1.770	347503.329

^a Under standard assumptions $E[Y(0)] = E[E[Y|A = 0, X]]$